BBA - Molecular Basis of Disease 1864 (2018) 2053–2066

Contents lists available at ScienceDirect

BBA - Molecular Basis of Disease

journal homepage: www.elsevier.com/locate/bbadis

Heterodimer formation by Oct4 and Smad3 differentially regulates epithelial-to-mesenchymal transition-associated factors in breast cancer progression

Gunjan Mandal[a], Subir Biswas[a], Sougata Roy Chowdhury[a], Annesha Chatterjee[a], Suman Purohit[a], Poulomi Khamaru[a], Sayan Chakraborty[a], Palash Kumar Mandal[b], Arnab Gupta[c], Jo-Anne de la Mare[d], Adrienne Lesley Edkins[d,*], Arindam Bhattacharyya[a,*]

[a] Immunology Laboratory, Department of Zoology, University of Calcutta, 35, Ballygunge Circular Road, Kolkata 700019, West Bengal, India
[b] Department of Pathology, College of Medicine and Sagore Dutta Hospital, B.T. Road, Kolkata, West Bengal, India
[c] Department of Surgical Oncology, Saroj Gupta Cancer Centre and Research Institute, Mahatma Gandhi Road, Kolkata, West Bengal, India
[d] Biomedical Biotechnology Research Unit, Department of Biochemistry and Microbiology, Rhodes University, Grahamstown 6140, South Africa

ARTICLE INFO

Keywords:
Breast cancer
EMT
Oct4
TGF-β
Smad3
Heterodimer

ABSTRACT

The multifunctional cytokine TGF-β crucially participates in breast cancer (BCa) metastasis and works differently in the disease stages, thus contributing in BCa progression. We address connections between TGF-β and the stem cell-related transcription factor (TF) Oct4 in BCa. In 147 BCa patients with infiltrating duct carcinoma, we identified a significantly higher number of cases with both moderate/high Oct4 expression and high TGF-β in late stages compared to early stages of the disease. *In vitro* studies showed that TGF-β elevated Oct4 expression, which in turn, regulated Epithelial-to-Mesenchymal transition (EMT)-regulatory gene (Snail and Slug) expression, migratory ability, chemotactic invasiveness and extracellular matrix (ECM) degradation potential of BCa cells. Putative binding sites for Oct4 on the snail, slug and cxcl13 promoters and for Smad3 on the snail and slug promoters were identified. Promoter activities of snail and slug were greater in dual-treated cells than only TGF-β-treated or Oct4-overexpressing cells. CXCL13 mRNA fold changes, however, were low in cells induced with TGF-β, compared to dual-treated or Oct4-overexpressing cells. Our co-IP studies confirmed that Oct4 and Smad3 form heterodimers that recognize specific promoter sequences to promote Snail and Slug expression, but which in turn, indirectly inhibits Smad3-mediated repression of CXCL13 expression, allowing Oct4 to act as a positive TF for CXCL13. Taken together, these data suggest that TGF-β signaling and Oct4 cooperate to induce expression of EMT-related genes Snail, Slug and CXCL13, which accelerates disease progression, particularly in the late stages, and may indicate a poor prognosis for BCa patients.

1. Introduction

Being one of the most frequently diagnosed diseases among women [1], breast cancer (BCa) accounts for increasing mortality worldwide [2], including India [3,4], where metastasis stands for maximum BCa-related deaths. Metastasis includes epithelial-to-mesenchymal transition (EMT), extracellular matrix (ECM) degradation, migration and invasion of tumor cells and other cell types to secondary metastatic site, leading to aggravating disease condition. Alterations in expression of epithelial and mesenchymal markers and EMT-regulatory transcription factors (TFs) occur during EMT [5,6]. Enhanced activity of Transforming Growth Factor-beta (TGF-β) and other growth factors elevates expression of EMT-regulators, thus promoting EMT [7–9]. TGF-β, a well-studied cytokine, plays important roles during cancer development

Abbreviations: BCa, Breast cancer; BLAST, Basic Local Alignment Search Tool; CCL5, –C-C motif ligand 5; CCR5, –C-C chemokine receptor type 5; ChIP, Chromatin immunoprecipitation; Co-IP, Co-immunoprecipitation; CSCs, Cancer stem cells; CXCL13, –CXC chemokine ligand 13; CXCR5, –CXC chemokine receptor 5; DAB, 3,3′-diaminobenzidine; Del, Deletion; ECM, Extracellular matrix; EMT, Epithelial-to-Mesenchymal Transition; ES, Early stage; ESC, Embryonic stem cells; H, High; h, Hours; IF, Immunofluorescence; IHC, Immunohistochemistry; L, Low; LNM, Lymph node metastasis; LS, Late stage; M/H, Moderate/High; MFI, Mean Fluorescence Intensity; min, Minutes; MMP, Matrix metalloproteinase; N/L, Negative/Low; NCBI, National Centre for Biotechnology Information; Oct4, Octamer-binding transcription factor 4; *p*-value, Probability value; PR, Progesterone receptor; qPCR, Quantitative PCR; RT, Room temperature; SGCC&RI, Saroj Gupta Cancer Centre and Research Institute; TGF-β, Transforming Growth Factor-beta; TF, Transcription factor; UICC, Union for International Cancer Control; WB, Western Blot

* Corresponding authors.
E-mail addresses: a.edkins@ru.ac.za (A.L. Edkins), arindam19@yahoo.com (A. Bhattacharyya).

https://doi.org/10.1016/j.bbadis.2018.03.010
Received 12 November 2017; Received in revised form 4 March 2018; Accepted 6 March 2018
Available online 08 March 2018
0925-4439/ © 2018 Elsevier B.V. All rights reserved.

and progression [10–12]. Studies have revealed that BCa early stages (ES) find TGF-β as a tumor suppressor, while in late stages (LS), it aids in cancer progression [13,14].

Additionally, increased/decreased activity of oncogenes or tumor suppressors contributes to disease manifestation, while, expression of these genes is regulated by TFs. TFs bind chiefly to promoter regions and influence transcription of specific genes [15,16]. Recent understanding of breast tumor biology points out the inherent potential of cancer stem cells (CSCs) for tumorigenesis [17,18], tumor relapse [19] and the process of metastasis [17]. Such a stem cell related-TF, Octamer-binding transcription factor 4 (Oct4) has been primarily reported for maintaining stem cell phenotype [20], self-renewal capacity [21–23] and pluripotency of embryonic stem cells (ESCs) [24,25], and also reported as CSC biomarker [21,26,27]. In addition, Oct4, solely or together with different TFs, potentiates tumorigenesis [26,27], regulates EMT [26], invasion [26,28], cancer progression [29,30], malignancy [31], poor prognosis and carcinogenesis of various cancers [31–36].

Besides this, TGF-β plays significant role in regulating fate and biology of ESCs [37]. Members of TGF-β family also determine cell migration in endometriosis by regulating Oct4 expression [38]. Recent studies have shown Smad3, downstream molecule of TGF-β signaling, to form complex with Oct4 which co-occupies the genome in ESCs [39,40]. TFs like Oct4 bound by Smad3 determine cell-type specific responses of TGF-β signaling [39,41].

Further, –CXC chemokine ligand 13 (CXCL13), a recent-discussed chemokine in the field of BCa progression, on binding to its cognate receptor –CXC chemokine receptor 5 (CXCR5) [42,43], helps in homing, migration and accumulation of B lymphocytes [42,44]. Expressed by many cell types, like follicular dendritic cells [45], macrophages [46] and germinal centre T cells [47], CXCL13 has been designated as a plasma biomarker of germinal centre activity [48], crucially participating in germinal centre formation [49]. This ligand-receptor pair plays crucial role in growth, attraction, invasion and migration in various cancers [50–52]. CXCL13 has been found over-expressed in both peripheral blood and tumor tissues of BCa patients with metastatic disease compared to normal patients [47]. Previously, we have shown this pair to potently induce EMT in BCa cells, by forming an autocrine loop, during lymph node metastasis (LNM) [53].

Presently, researchers have identified putative connections of TGF-β with both Oct4 and CXCL13. Some reports state that a subset of human CD4+ T cells produce CXCL13 in rheumatoid synovium cell types [54,55], where TGF-β plays role in differentiation of these CXCL13-producing CD4+ T cells from naive CD4+ T cells in ectopic lymphoid-like-structure cells [56]. On the other hand, TGF-β induces Oct4-up-regulation in undifferentiated ESCs in a Smad-mediated mechanism [57]. We hypothesize that TGF-β signaling may be directly linked with Oct4 in driving EMT and metastasis of BCa cells. Our bioinformatics analyses found Oct4 and/or Smad3-binding sites to encompass proximal promoter regions of snail, slug and cxcl13. In this study, we establish a relationship between Oct4 and Smad3 in connection to Snail-Slug-mediated and CXCL13-mediated BCa progression. This study is novel because it highlights the differential association between Oct4 and Smad3 in regulating Snail, Slug and CXCL13. It also indicates a potential mechanism to explain the contrasting role of TGF-β in BCa ES and LS.

2. Results

2.1. Correlation of Oct4 expression with TGF-β expression in primary breast tumor tissues

We have analyzed Oct4 and TGF-β expression in primary breast tumor and adjacent healthy normal tissues (Table 1; Supplementary Table S1). The mRNA fold changes ($2_T^{-\Delta\Delta C}$) < 4 has been considered as "Low or L" for TGF-β and "Negative/Low or N/L" for Oct4, while, $2_T^{-\Delta\Delta C} \geq 4$ as "High or H" for TGF-β and "Moderate/High or M/H" for Oct4. Grouping samples according to TGF-β and Oct4 expression exhibited that 37.37% ($n = 52$) tumor samples express TGF-β-H/Oct4-M/H, whereas, 25.85% ($n = 38$) express TGF-β-L/Oct4-N/L (Fig. 1A, Table 2). More precisely, TGF-β-H samples ($n = 86$) displayed a median Oct4 ΔC_T-value of 5.0, significantly lower ($p < 0.05$) than TGF-β-L samples ($n = 61$) which is 12.4 (Fig. 1B). This clearly indicates that within the primary breast tumors, higher the TGF-β expression, higher is the Oct4 level. Chi-square test has determined that there is a significant ($p = 0.00653$) association between TGF-β and Oct4 expression.

Table 1
Clinicopathological characteristics of patients with various expression grades of Oct4, TGF-β and CXCL13.

Characteristics	Number of patients per group
Total	147
Age (median and range) in years	47 (23–78)
pT status	
pT_1	21
pT_2	77
pT_3	39
pT_4	10
pN status	
pN_0	59
pN_1	27
pN_2	34
pN_3	27
M status	
M_0	122
M_1	17
M_X	8
Stage	
Early [I + II]	86
Late [III + IV]	61
Tumor differentiation grade	
Well (I)	18
Moderate (II)	69
Poor (III)	60
TGF-β fold change	
< 4 (Low)	61
≥4 (High)	86
Oct4 expression grade	
Negative	15
Low	57
Moderate	15
High	60
CXCL13 expression grade	
Negative	36
Low	43
Moderate	9
High	33

2.2. TGF-β induces elevated Oct4 expression in BCa cells and immortalized normal breast cells

With reports demonstrating TGF-β signaling regulating Oct4 expression [38], we examined the Oct4-inducing potential of TGF-β *in vitro*. BCa cell lines, MCF7 and MDA-MB-231, and immortalized normal breast epithelial cell line MCF10A were treated with recombinant TGF-β1. qPCR showed a considerable increase in Oct4 mRNA expression in TGF-β-treated cells (Fig. 2A). In 0.5 and 1.0 ng/mL-TGF-β-treated cells, Oct4 $2_T^{-\Delta\Delta C}$ were 6.69 ($p < 0.001$) and 11.52 ($p < 0.001$), respectively in MCF7; 8.69 ($p < 0.001$) and 13.62 ($p < 0.001$), respectively in MDA-MB-231; and 5.42 ($p < 0.001$) and 8.35 ($p < 0.001$), respectively in MCF10A (Fig. 2A). Correspondingly, we observed significantly elevated Oct4 protein levels in TGF-β-induced cells (Fig. 2B and C).

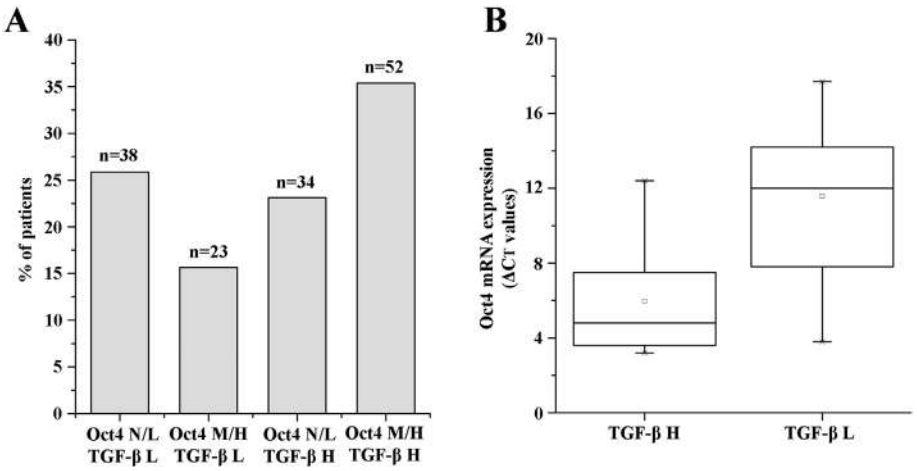

Fig. 1. Correlation of TGF-β and Oct4 expression within primary breast tumor.
(A) Number of samples (represented as percentages) that express negative or low Oct4 (Oct4-N/L) and low TGF-β both (TGF-β-L) is 38, number of samples that express moderate or high Oct4 (Oct4-M/H) and TGF-β-L is 23; number of samples that express Oct4-N/L and high TGF-β (TGF-β-H) is 34; and number of samples that express Oct4-M/H and TGF-β-H is 52. The mRNA fold changes ($2_T^{-\Delta\Delta C}$) < 4 has been considered as "Negative/Low" for Oct4 and "Low" for TGF-β, whereas, mRNA fold changes ≥4 has been considered as "Moderate/High" for Oct4 and "High" for TGF-β. (B) Box plot showing ΔC_T values (C_T value of Oct4 – C_T value of 18S rRNA) of Oct4 mRNA expressions in TGF-β-H and TGF-β-L samples. Median ΔC_T value of Oct4 mRNA expression in TGF-β-H samples is 5.0 and in TGF-β-L samples is 12.4.

Table 2
Expression status of CXCL13 relative to expressions of Oct4 and TGF-β in primary breast tissue specimens.

	Total	CXCL13 N/L	CXCL13 M/H
Oct4-L - TGF-β N/L	38	37	1
Oct4-H - TGF-β N/L	23	3	20
Oct4-L - TGF-β M/H	34	33	1
Oct4-H - TGF-β M/H	52	6	46

2.3. TGF-β-induced Oct4-overexpression is not restricted to $CD44^{high}CD24^{low/negative}$ stem cells

Oct4 is considered as a stemness marker [20–27] and regulates CSC activity towards disease progression [20–28]. We observed that TGF-β elevates Oct4 production in MCF7 and MDA-MB-231 cells (Fig. 2). Both cell lines contain a considerable percentage of $CD44^{high}CD24^{low/negative}$ cells, thought to represent CSCs [58].On performing flow cytometry, we found TGF-β-induced Oct4-overexpression was not limited to CSCs only, but happened in remaining non-stem cells too (Fig. 3).

2.4. Oct4 and TGF-β signaling regulate EMT-regulators and matrix metalloproteinases (MMPs)

Role of Oct4 as TF to regulate EMT-pathways has been debated [59,60]. Cells were treated in different combinations with recombinant TGF-β1, Oct4-overexpression plasmid, Oct4-siRNA and Smad3-siRNA (Supplementary Fig. S1). TGF-β-treated cells demonstrated significant mRNA fold increase in EMT-regulators Snail and Slug, mesenchymal markers Vimentin and N-cadherin, MMPs-MMP2 and MMP9 and significant decrease in epithelial marker E-cadherin expression (Fig. 4A). Oct4-overexpression demonstrated similar results except mRNA fold

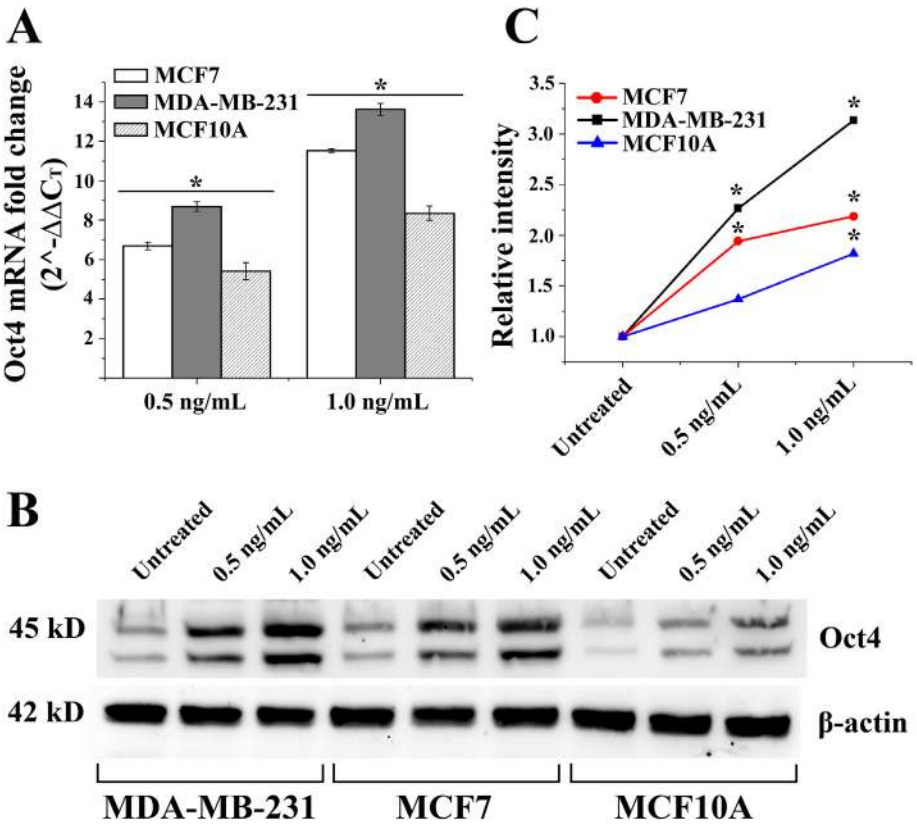

Fig. 2. Analyses of Oct4 expression in TGF-β-induced breast cancer and normal breast cell lines.
MCF7, MDA-MB-231 and MCF10A cell lines were treated with recombinant human TGF-β1 at 0.5 and 1.0 ng/mL concentrations. (A) Quantitative real-time PCR for Oct4 was performed. Fold changes are represented as relative values normalized to the 18S rRNA control. (B) Protein levels of Oct4 were evaluated by western blot analysis. β-actin was used as loading control. (C) Densitometry of the Oct4 signal in the western blot in 2B. Relative intensities for Oct4, normalized to the β-actin loading control, were calculated using ImageJ software and are shown in line graphs. Results are representative of three independent experiments performed in triplicate and are represented as mean ± SEM. One-way ANOVA with Bonferroni correction was performed, using Origin8 software, to determine statistical significance, where $^*p \leq 0.05$.

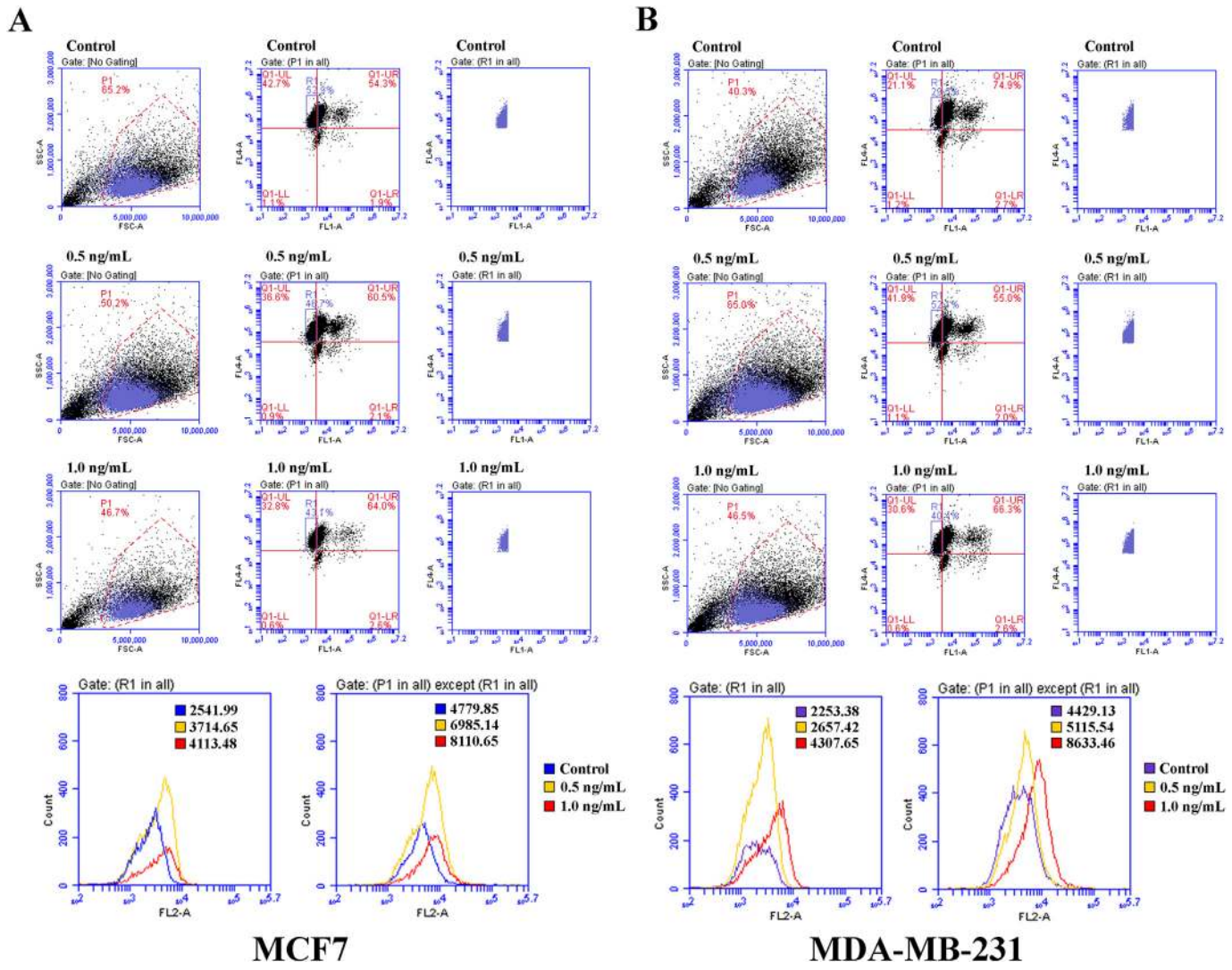

Fig. 3. TGF-β-stimulation induces Oct4 expression in $CD44^{high}CD24^{low/negative}$ and bulk cell populations.
(A) MCF7 and (B) MDA-MB-231 cells were treated with recombinant human TGF-β1 at 0.5 and 1.0 ng/mL concentrations. Flow cytometry was performed after incubating single cell suspensions with Alexa Fluor488-anti-CD44, Alexa Fluor647-anti-CD24 and PE-anti-Oct4. Cells with a central tendency were P1-gated from FSC-A *vs*. SSC-A. $CD44^{high}CD24^{low/negative}$ CSCs were gated as R1 from P1-gated-FL1 (Alexa Fluor488) *vs*. FL4 (Alexa Fluor647). Mean Fluorescence Intensity (MFI) values of PE (FL2) in the R1-gated population and in the P1-gated population excluding R1 were analyzed from FL2 *vs*. count histograms. Results are representative of three independent experiments performed in triplicate. In untreated, 0.5 and 1.0 ng/mL-treated MCF7 cells, MFI values of Oct4-PE (FL2) in R1-gated CSC population were 2541.99, 3714.65, 4113.48, respectively and in R1-excluded non-stem cells were 4779.85, 6985.14, 8110.65, respectively. In MDA-MB-231, MFI values in R1-gated population were 2253.38, 2657.42, and 4307.65, respectively and in R1-excluded cells were 4429.13, 5115.54, 8633.46, respectively.

changes of N-cadherin and Vimentin, which were not significant. Correspondingly, Smad3-silencing showed significant decrease in Snail, Slug, Vimentin, N-cadherin, MMP2, MMP9 expression, and increase in E-cadherin expression; while, Oct4-knockdown resulted in significantly decreased Snail, Slug, MMP2, MMP9 and increased E-cadherin. Most importantly, simultaneous induction by Oct4-overexpression and TGF-β resulted in further increase in Snail and Slug expression (27.47 and 32.22 fold for Snail; 28.25 and 24.76 fold for Slug in MCF7 and MDA-MB-231 cells, respectively) significantly higher than that observed for individual treatments (Fig. 4A). No such cumulative effects were observed for Vimentin and N-cadherin. BCa cells also express elevated Snail and Slug protein upon either Oct4-overexpression or TGF-β-treatment (Fig. 4B), and even higher on receiving simultaneous induction (Fig. 4C). Altogether, these data support our observation that both TGF-β and Oct4 regulate Snail, Slug, MMP2, MMP9 and E-cadherin transcription independently, while having a synergistic effect when combined.

2.5. Increased migration and chemotactic invasion by Oct4-overexpressing BCa cells

Cancer starts spreading to secondary sites when tumor cells invade ECM [61,62]. Our observation of increased MMP2, MMP9 production by Oct4-overexpressing BCa cells indicated possible increase in their migration and chemotactic invasion potential. On performing wound-healing assay, we observed significantly faster wound closure in Oct4-overexpressing BCa cells compared to untreated cells (Fig. 5A). This indicated that Oct4-overexpression accelerated migration rate of BCa cells, possibly because of EMT and increased MMP2/9 production.

Further, chemotactic invasion potential of control and Oct4-overexpressing MDA-MB-231 cells was estimated using agarose spot assay. We used chemoattractant –C-C motif ligand 5 (CCL5) (25 ng/mL) in the agarose spots for migrating MDA-MB-231 cells, expressing –C-C chemokine receptor type 5 (CCR5). We observed that, Oct4-overexpressing MDA-MB-231 cells showed higher agarose invasion after 24 h, compared to control cells (Fig. 5B). Cells were unable to invade agarose

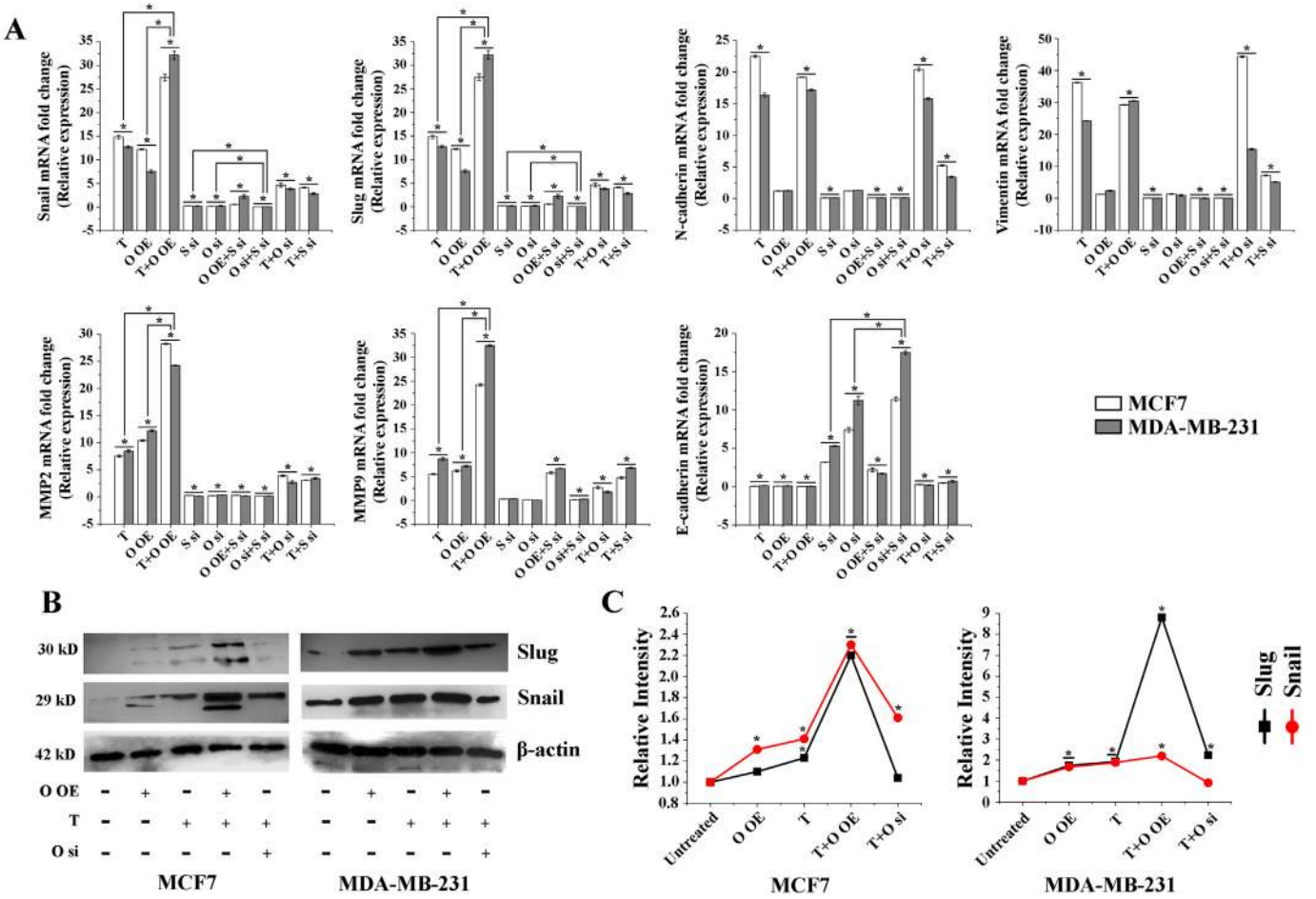

Fig. 4. Alterations in the expression of EMT markers and regulators in response to TGF-β and Oct4 levels.
T represents cells treated with 1.0 ng/mL recombinant TGF-β1. O OE represents cells transfected for Oct4 overexpression, S si represents cells transfected with Smad3 siRNA, O si represents cells transfected with Oct4 siRNA. (A) Fold changes ($2^{-\Delta\Delta C}_{T}$) of mRNA expression of Snail, Slug, N-cadherin, E-cadherin, Vimentin, MMP2 and MMP9 relative to untreated cells were calculated and represented as bar graphs. (B) Western blot analyses of Snail and Slug. β-actin was used as loading control. (C) Densitometry analyses of bands in B, using ImageJ software, represented as line graphs. Results are representative of three independent experiments performed in triplicate and are represented as mean ± SEM. One-way ANOVA with Bonferroni correction was performed, to assess statistical significance, where $^{*}p \leq 0.05$.

spots lacking CCL5. This clearly indicated that Oct4-overexpression imparted increased chemotactic invasion ability to the BCa cells.

2.6. Activation of MMP2 and MMP9

Active MMP2 and MMP9 are known to promote ECM degradation and metastasis during BCa [63,64]. Gelatin zymogram indicated that TGF-β-treated BCa cells show limited increase in MMP2/9 activity (Fig. 5C). However, this increase was higher and significant ($p < 0.05$) in Oct4-overexpressing cells. Correspondingly, cells that received combined stimulation showed even higher MMP2/9 activities (Fig. 5C).

2.7. Oct4 and Smad3 both regulate snail and slug promoter activities

It has previously been reported that Smad3 and Oct4 co-occupy some genomic regions, particularly promoters, thereby, influencing transcription of many genes [39,40]. To address the synergistic effect of TGF-β signaling and Oct4 in regulating Snail and Slug expression, we analyzed snail (−863/+280) and slug (−1015/+375) promoter regions, where both have one probable binding site, each for Smad3 and Oct4 (Fig. 6, Supplementary Figs. S2 and S3). Genomic fragments of snail and slug promoters were sub-cloned, upstream of the luciferase gene in pGL3 basic reporter vector. Promoter activity was quantified in terms of luciferase mRNA fold change.

In TGF-β-induced MCF7 and MDA-MB-231 cells, luciferase mRNA fold changes for snail promoter were 18.74 and 22.61, respectively (Fig. 6A). Oct4-overexpressing MCF7 and MDA-MB-231 cells had fold changes of 22.34 and 24.46, respectively (Fig. 6A). Promoter activities of slug were also found to be sensitive to both TGF-β-mediated stimulation (14.55 and 16.34 in MCF7 and MDA-MB-231 cells, respectively) as well as Oct4-overexpression (18.67 and 17.42 in MCF7 and MDA-MB-231 cells, respectively) (Fig. 6B). Interestingly, similar to our qPCR result, snail and slug promoter activities were elevated many fold when cells were treated simultaneously with Oct4-overexpression and TGF-β (38.61 and 49.34 for snail; 25.21 and 23.66 for slug in MCF7 and MDA-MB-231 cells, respectively) (Fig. 6).

2.8. Promoter regions of snail and slug contain Oct4 and Smad3 responsive regions

We designed 7 deletion variants of snail promoter (Del1–863/−749; Del2–863/−620; Del3–863/−484; Del4–863/−352; Del5–863/−204; Del6–863/−30; Del7–863/+92) and 9 slug promoter variants (Del1–1015/−887; Del2–1015/−719; Del3–1015/−633; Del4–1015/−470; Del5–1015/−351; Del6–1015/−205; Del7–1015/−37; Del8–1015/+102; Del9–1015/+269) to methodically identify regions responsible for Oct4-mediated and TGF-β-mediated regulation of snail and slug transcription in BCa cell lines (Fig. 6). Promoter activity was also quantified by measuring luciferase mRNA fold changes.

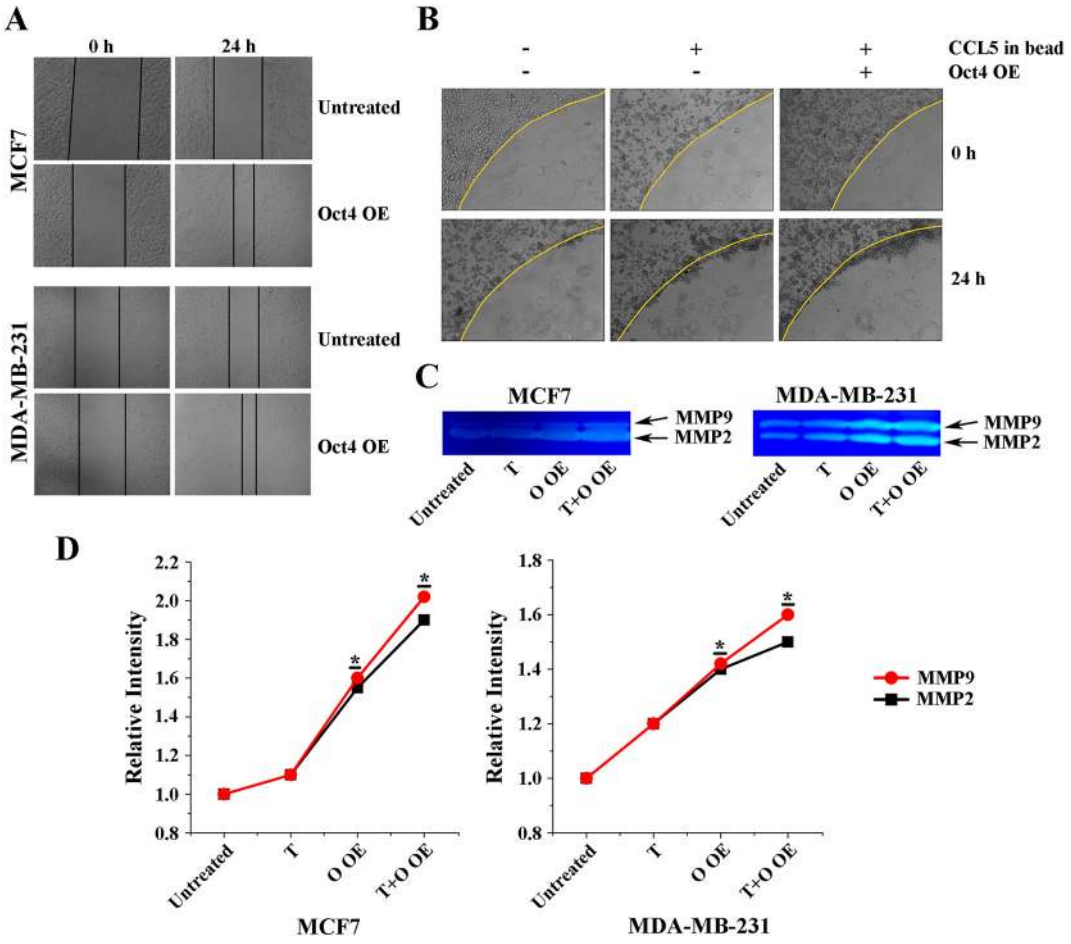

Fig. 5. Analyses of migration, invasion and MMP2/9 activities in breast cancer cell lines.
(A) To examine relative migration of control and Oct4-overexpressing breast cancer cell lines, wounds were made in cell layers, immediately prior to transfection with Oct4 (Oct4 OE). Wound closure was observed after 24 h in with a phase contrast microscope (Zeiss Aixovert 40C) with 50× magnification. (B) CCL5-dependent chemotactic invasion of MDA-MB-231 cells upon Oct4-overexpression (Oct4 OE) was observed by agarose spot assay. (C) Gelatin zymogram showing enzymatic activities of MMP2 and MMP9 in both cell lines. T indicates treatment with 1.0 ng/mL recombinant TGF-β1, O OE indicates Oct4 overexpression and T + O OE indicates a combination of both 1.0 ng/mL TGF-β1 treatment and Oct4 overexpression. (D) Relative intensities of the MMP2/9 bands were measured, using ImageJ software and are represented in line graphs. Results are representative of three independent experiments performed in triplicate and are represented as mean ± SE. One-way ANOVA with Bonferroni correction was performed to determine statistical significance, where $^{*}p \leq 0.05$.

For snail promoter, in TGF-β-treated cells, all deletions, except Del1, resulted in significant decrease in promoter activity. However, Del1 led to significant reduction in snail promoter activities in Oct4-overexpressing, dual-treated and untreated cells. Importantly, in Del2, we observed complete loss of any significant difference in snail promoter activities between differently-treated and untreated cells (Fig. 6A). These data indicate that Oct4 has a binding site within the deleted region of Del1, positioned between −863 to −749 (Supplementary Fig. S2) whereas, Smad3 may bind within the deleted region of Del2, and thereby regulate snail promoter transcription.

Considering slug promoter activities in TGF-β-treated cells, the first significant decrease in luciferase signal was observed in Del8. In Oct4-overexpressing cells, all deletions, starting from Del1, resulted in noteworthy decreases in slug promoter activities in both the cell lines. Correspondingly, in dual-induced cells, significant decrease in luciferase signal in Del1 and an almost complete loss in transcriptional activity in Del8 were observed (Fig. 6B). Data supports bioinformatics prediction that a probable Oct4 binding site within the deleted region of Del1, positioned between −1015 to −887, and Smad3 binding site within the deleted region of Del8, positioned between −36 to +102 (Supplementary Fig. S3).

2.9. Oct4 and TGF-β signaling play converse roles in regulating CXCL13 expression

It is known that CXCL13 signaling is associated with EMT of BCa cells [53]. Cxcl13 promoter region has three putative binding sites for Oct4 (Supplementary Fig. S4). Oct4-overexpression induced CXCL13 mRNA expression in both MCF7 (47.5 fold) and MDA-MB-231 (45.25 fold) cells. Interestingly, TGF-β-treated cells had significantly decreased CXCL13 mRNA expression (0.36 and 0.22 fold in MCF7 and MDA-MB-231, respectively). Furthermore, cells that received combined stimulation with TGF-β and Oct4-overexpression showed significant reduction in CXCL13-upregulation (12.04 and 8.57 fold in MCF7 and MDA-MB-231, respectively) compared to cells with Oct4-overexpression alone. Most surprisingly, Smad3-knockdown resulted in significantly increased CXCL13 mRNA expression. This finding is intriguing since the cxcl13 promoter does not contain any predicted Smad3 binding site. Silencing of Oct4, confirmed that Oct4 positively regulated CXCL13 expression. Maximum fold change was observed where Oct4-overexpression and Smad3-silencing was done (Fig. 7A).

CXCL13 protein levels were also maximal in Oct4-overexpressed and Smad3-silenced cells (132.78 and 141.2 pg/mL in MCF7 and MDA-MB-231 cells, respectively) (Fig. 7B), whereas, sole-Smad3-knockdown was associated with increased CXCL13 (68.55 and 87.25 pg/mL in

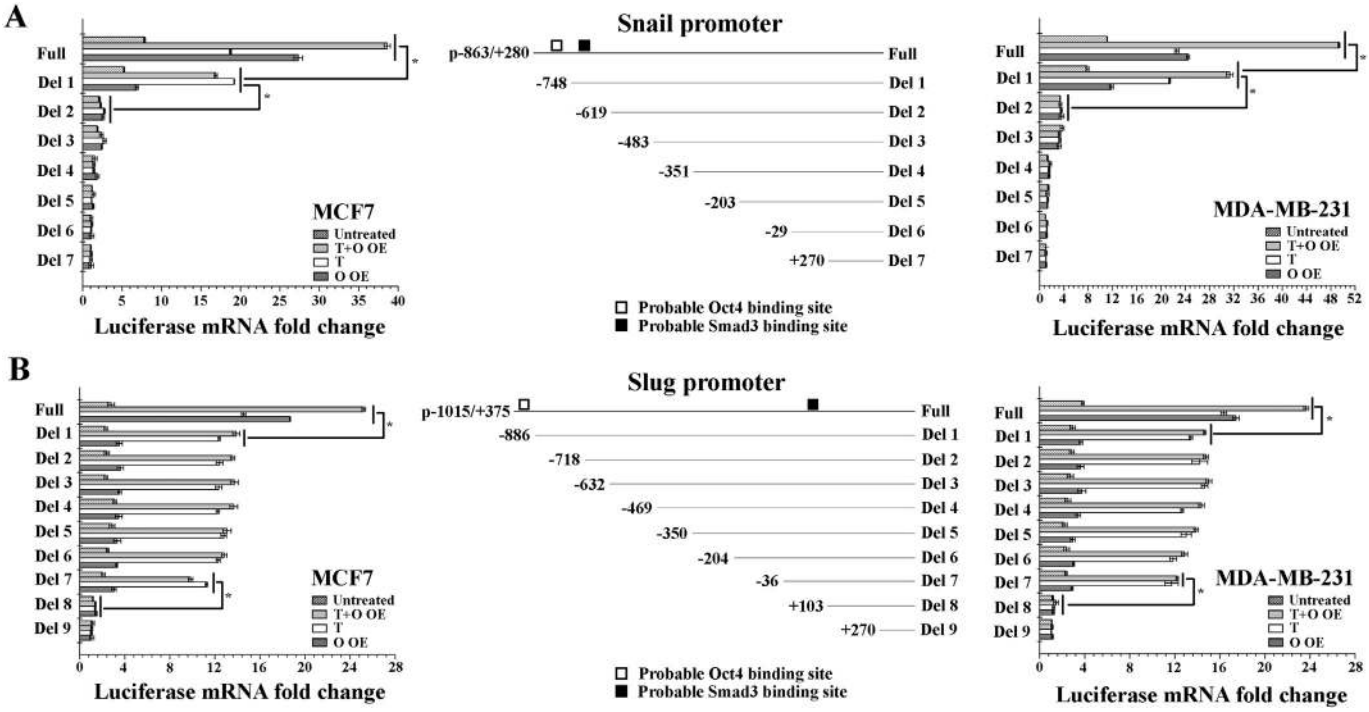

Fig. 6. Oct4 and Smad3-mediated regulation of Snail and Slug promoter activities.
(A) Functional analysis of deletion scanning of Snail promoter. Locations of the deletions on the Snail promoter map are shown in the middle panel. Positions of putative binding sites of Oct4 (white) and Smad3 (black) are indicated as boxes. Luciferase mRNA fold-changes ($2^{-\Delta\Delta C}_{T}$) in MCF7 (left) and MDA-MB-231 (right) cells are represented as bar graphs. (B) Functional analysis of deletion scanning of Slug promoter. Locations of the deletions on the Slug promoter map are shown in the middle panel. Positions of putative binding sites of Oct4 (white) and Smad3 (black) are indicated as boxes. Luciferase mRNA fold-changes ($2^{-\Delta\Delta C}_{T}$) in MCF7 (left) and MDA-MB-231 (right) cells are represented as bar graphs. T represents cells treated with 1.0 ng/mL recombinant TGF-β1. O OE represents cells transfected for Oct4 overexpression. Results are representative of three independent experiments performed in triplicate and are represented as mean ± SEM. One-way ANOVA with Bonferroni correction was performed to assess statistical significance, where $^{*}p \leq 0.05$.

MCF7 and MDA-MB-231 cells, respectively). The lowest CXCL13 concentration was observed when TGF-β-stimulation and Oct4-knockdown was done (Fig. 7B). Collectively, these results led us to hypothesize that TGF-β signaling imposes a negative regulatory effect on cxcl13 transcription, while, on the contrary, Oct4 acts as a positive regulator for the same.

2.10. Oct4 positively regulate cxcl13 transcription

The genomic fragment of the cxcl13 promoter (−2000/+301) was sub-cloned in pGL3 vector. In Oct4-overexpressing cells, we observed significant increase in luciferase mRNA fold change (23.49 fold in MCF7 and 21.3 in MDA-MB-231 cells). Interestingly, we did not observe any significant decrease in cxcl13 promoter activity upon TGF-β-treatment. Untreated MCF7 and MDA-MB-231 cells demonstrated 3.54 and 5.13 fold changes, respectively whereas, TGF-β-treated cells showed 4.3 and 4.84, respectively. Surprisingly, BCa cells co-stimulated with TGF-β and Oct4 demonstrated higher luciferase signal (30.54 and 28.78 fold in MCF7 and MDA-MB-231 cells, respectively) than Oct4-overexpressing cells (Fig. 7C). We hypothesize that, in presence of Oct4, the inhibitory pathway induced by TGF-β is somehow turned off. On the contrary, TGF-β induces Oct4 expression, which may, in turn, increases Oct4-induced-cxcl13 promoter activity.

2.11. Promoter region of cxcl13 contain Oct4 responsive regions

We designed 14 deletion variants of cxcl13 promoter (Del1–2000/−1679; Del2–2000/−1439; Del3–2000/−1288; Del4–2000/−1103; Del5–2000/−801; Del6–2000/−688; Del7–2000/−564; Del8–2000/−462; Del9–2000/−319; Del10–2000/−218; Del11–2000/−109; Del12–2000/−15; Del13–2000/+148; Del14–2000/+217) to identify responsive regions (Fig. 7C). We identified three putative binding sites for Oct4, but no site for Smad3, within the cxcl13 promoter region. The first, second and third Oct4 binding sites are positioned in the deleted regions of Del1, Del3 and Del4, respectively.

Significant reduction in Oct4-induced luciferase signal was observed in Del1, however, it retained most of the fold change (23.49 and 18.6 in Full and Del1, respectively, in MCF7; 21.3 and 16.62 in Full and Del1, respectively, in MDA-MB-231). A second drastic decrease in fold change was observed in Del3 (17.56 and 4.14 in Del2 and Del3, respectively, in MCF7; 16.67 and 3.78 in Del2 and Del3, respectively, in MDA-MB-231) with further decrease in Del4 (Fig. 7C). These results indicate that the second Oct4-binding site has the maximum influence followed by the first in cxcl13 transcription. Though a gradual decrease in luciferase signal is also observed in TGF-β-stimulated cells, this may be due to elimination of the Oct4 binding sites from the promoter.

2.12. Oct4 forms heterodimer with Smad3

We next examined how TGF-β-mediated-CXCL13 downregulation is repressed in presence of Oct4. BLAST-analyses showed considerable alignment between Oct4 and Smad3, which suggested that they may form a heterodimer (Supplementary Fig. S5). Thus, we hypothesized that Oct4 may sequester Smad3 and thereby hamper TGF-β-mediated-downregulation of CXCL13 expression.

Co-immunoprecipitation (Co-IP) studies demonstrated that Oct4-knockdown resulted in significant decrease of Smad3 in Oct4-immunoprecipitates (Fig. 8A and B). Correspondingly, Oct4-overexpression led to increased Smad3 in the anti-Oct4-IP protein fraction (Fig. 8A). Importantly, either of Oct4-overexpression or knockdown did not show any considerable effect on Smad3 levels in the input, whereas, Smad3-knockdown led to reduced input-Smad3 level which was also

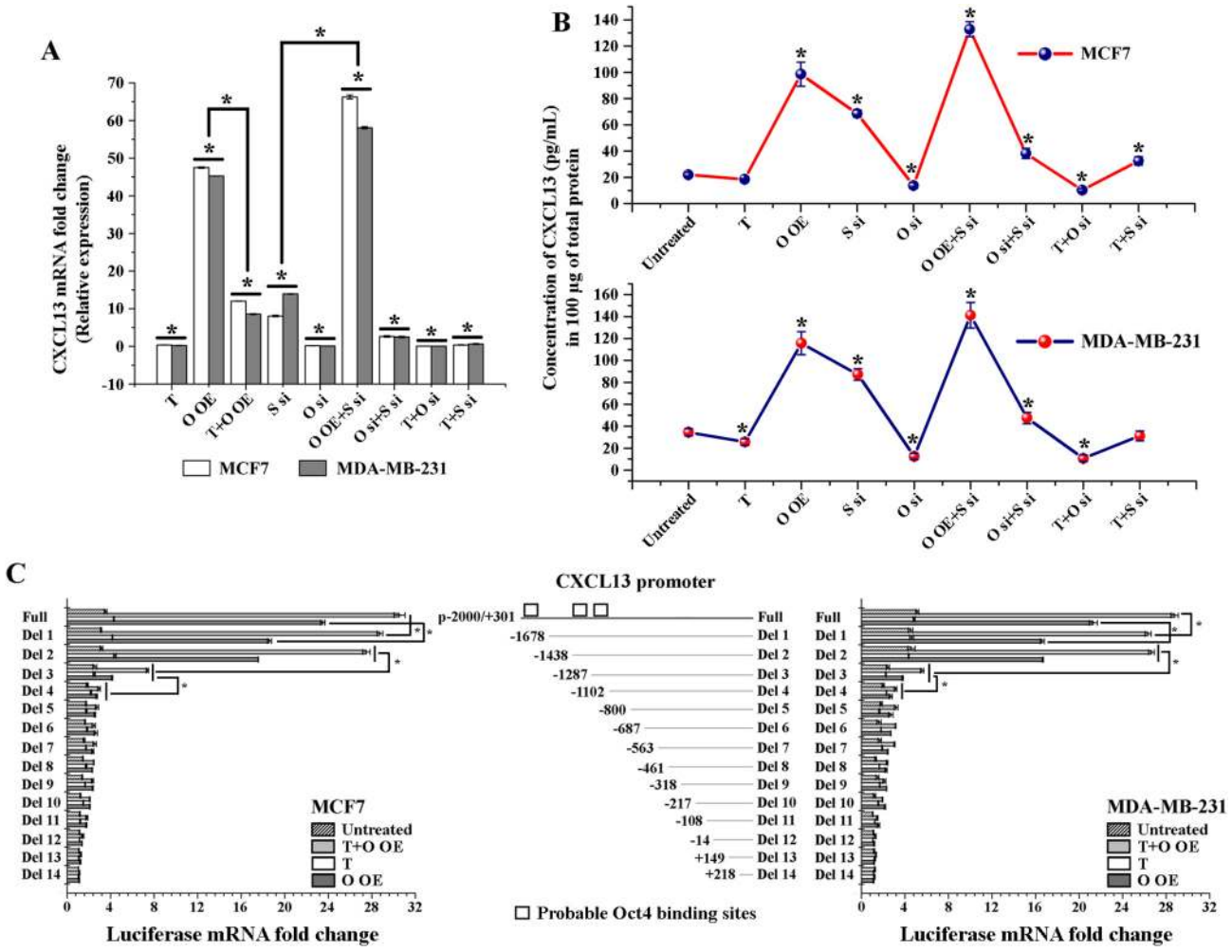

Fig. 7. Regulation of CXC13 expression by Oct4 and TGF-β.
(A) Fold changes ($2_T^{-\Delta\Delta C}$) of CXCL13 mRNA expression relative to untreated cells was calculated and represented as bar graphs. (B) Quantitative CXCL13 protein concentrations (pg/mL) in 100 µg of total protein were measured by ELISA and are represented as line graphs. (C) Functional analysis of deletion scanning of CXCL13 promoter. Locations of the deletions on the CXCL13 promoter map are shown in the middle panel. Positions of putative binding sites of Oct4 (white) are also indicated. Luciferase mRNA fold-changes ($2_T^{-\Delta\Delta C}$) in MCF7 (left) and MDA-MB-231 (right) cells are represented as bar graphs. T represents cells treated with 1.0 ng/mL recombinant TGF-β1. O OE represents cells transfected for Oct4 overexpression, S si represents cells transfected with Smad3 siRNA, O si represents cells transfected with Oct4 siRNA. Results are representative of three independent experiments performed in triplicate and are represented as mean ± SEM. One-way ANOVA with Bonferroni correction was performed to assess statistical significance, where $^*p \leq 0.05$.

evident in the Oct4-immunoprecipitates. TGF-β treatment resulted in increased Smad3 in the anti-Oct4-IP protein fraction (Fig. 8A and B).

Further, time-dependent studies in Oct4-overexpressing cells demonstrated that Smad3-binding with Oct4 increases gradually from 0 h to 24 h post-transfection. Smad3-input levels were comparable at all time-points, whereas, Oct4-overexpression attained saturation within the first 6 h of transfection (Fig. 8C). Relative intensities of anti-Oct4-IP:Smad3-western blot (WB) bands at 6 h, 12 h and 24 h are 1.74, 1.71, 1.9, respectively in MCF7; 1.4, 1.8, 1.9, respectively in MDA-MB-231 cells (Fig. 8D). These results cumulatively indicate that Oct4 binds to Smad3 and forms heterodimer.

2.13. Oct4 and Smad3 bind to snail and slug promoter

To verify *in vivo* Oct4 and Smad3 binding to snail and slug promoter, we performed conventional Chromatin immunoprecipitation (ChIP) assay. We designed 2 amplicons from the snail promoter. Amplicon-1 comprises Oct4 and Smad3 binding sites, while amplicon-2 is distantly located from both the sites (Fig. 9A). For the slug promoter, we designed 3 amplicons. Amplicon-1 comprises Oct4 binding site, amplicon-2 comprises Smad3 binding site, while amplicon-3 is distantly located from both the sites (Fig. 9B). Considering snail promoter, amplicon-1 produced much stronger signals than amplicon-2 for all treatment conditions for both anti-Oct4 and anti-Smad3 IP (Fig. 9A). Comparing untreated cells with Oct4-overexpressing and TGF-β-treated cells, the anti-Oct4-IP showed the highest amplicon-1 signal in Oct4-overexpressing cells, followed by TGF-β-treated cells, whereas, for anti-Smad3-IP, TGF-β-treated cells had the highest amplicon-1 signal (Fig. 9A).

For slug promoter, amplicon-1, but not amplicon-2 and amplicon-3, showed stronger signal for anti-Oct4-IP (Fig. 9B). Correspondingly, for anti-Smad3-IP, only amplicon-2 showed stronger signal (Fig. 9B). Among anti-Oct4-IP samples, amplicon-1 had the highest signal in Oct4-overexpressing cells, as compared to untreated and TGF-β-treated cells. Likewise, the anti-Smad3-IP showed the highest signal in TGF-β-treated cells (Fig. 9B).

2.14. Oct4 binds to cxcl13 promoter

ChIP-analyses was performed to verify *in vivo* Oct4 binding to CXCL13 promoter. We designed 4 amplicons from the cxcl13 promoter: amplicon-1 contains first Oct4 binding site, amplicon-2 contains second

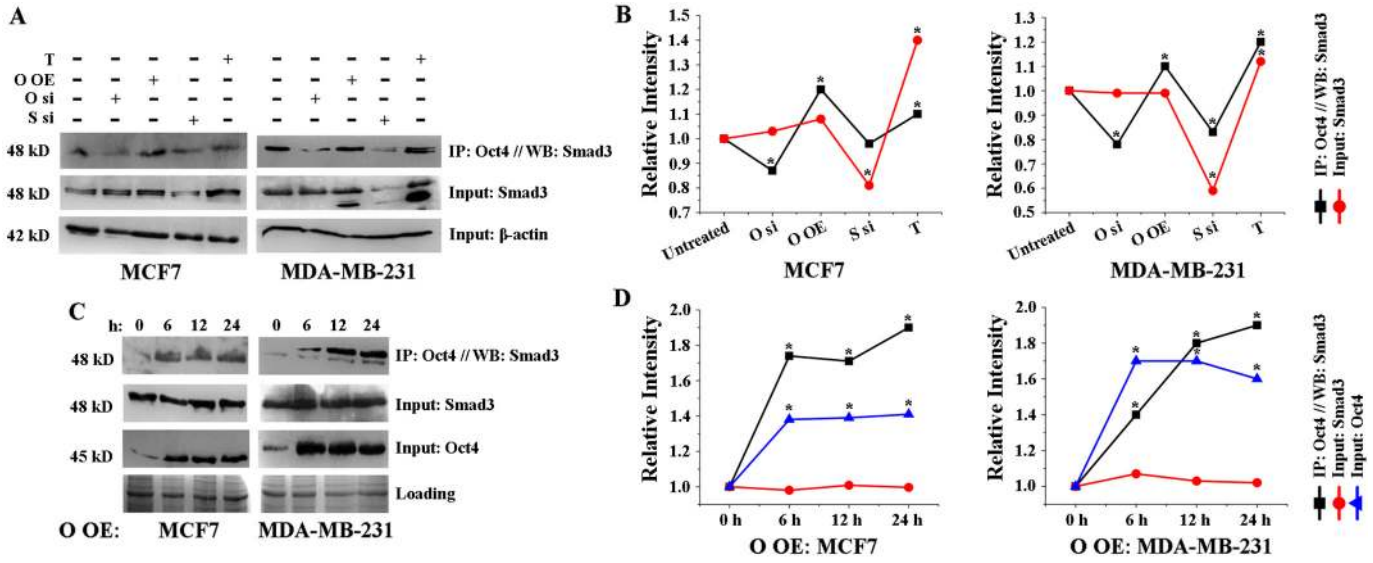

Fig. 8. Heterodimer formation by Oct4 and Smad3.
(A) Western blot analyses of Smad3 in immuno-precipitated (IP) samples using anti-Oct4 antibody in MCF7 and MDA-MB-231 cells. T represents cells treated with 1.0 ng/mL recombinant TGF-β1. O OE represents cells transfected for Oct4 overexpression, S si represents cells transfected with Smad3 siRNA, O si represents cells transfected with Oct4 siRNA. Input Smad3 bands were developed using total crude protein samples. β-actin was used as loading control. (B) Relative intensities were calculated from densitometry analyses of bands, using ImageJ software and are represented as line graphs. (C) Time dependent dimer formation was analyzed by IP using anti-Oct4 antibodies at 0 h, 6 h, 12 h and 24 h post-transfection and subsequent western blot using anti-Smad3 antibodies. Input Smad3 and Input Oct4 bands were developed using total crude protein samples. β-actin was used as loading control. (D) Relative intensities of bands from time dependent IP studies were calculated from densitometry analyses of bands using ImageJ software and are represented as line graphs. Results are representative of three independent experiments performed in triplicate and are represented as mean ± SEM. One-way ANOVA with Bonferroni correction was performed to determine statistical significance, where $^{*}p \leq 0.05$.

Oct4 binding site, and amplicon-3 contains third Oct4 binding site, while, amplicon-4 is distantly located from all of the three Oct4 binding sites (Fig. 9C). ChIP analyses showed amplicon-2 has strongest signal in all treatment conditions, followed by amplicon-1 and then amplicon-3 (Fig. 9C). Amplicon-4 did not show any considerable signal. Signals from all amplicons, except amplicon-4, showed strongest signal in Oct4-overexpressing cells, followed by TGF-β-treated cells (Fig. 9C).

Additionally, Immunofluorescence (IF) analyses of breast tumor tissues have clearly indicated considerable co-localization of Smad3 and Oct4 (Fig. 9D).

2.15. Expression of EMT-regulators, markers, MMPs and CXCL13 in breast tumor tissues

Tumor tissues were categorically divided in four sub-groups: Oct4-N/L-TGF-β-L, Oct4-N/L-TGF-β-H, Oct4-M/H-TGF-β-L and Oct4-M/H-TGF-β-H. Variables were analyzed by Kolmogorov-Smirnov test which found that they did not follow normal distribution. Therefore, Mann-Whitney *U* test was performed to study association between patient sub-groups and mRNA expression of Snail, Slug, N-cadherin, Vimentin, E-cadherin, MMP2, MMP9, and CXCL13. Resulted *p*-values are represented as a scatter plot to understand the significance of fold change of the genes between sub-groups: Oct4-N/L-TGF-β-L *vs.* Oct4-N/L-TGF-β-H (Fig. 10A), as well as between Oct4-M/H-TGF-β-L *vs.* Oct4-M/H-TGF-β-H (Fig. 10B).

Statistically significant overexpression of Snail ($p = 1.40E^{-12}$), Slug ($p = 1.40E^{-12}$), Vimentin ($p = 3.87E^{-06}$), MMP2 ($p = 0.00083$), and MMP9 ($p = 0.000025$) was only observed in Oct4-N/L-TGF-β-H tissues. E-cadherin fold decrease was significant ($p = 4.10E^{-11}$) in Oct4-N/L-TGF-β-H tissues but not ($p = 0.31095276$) in Oct4-N/L-TGF-β-L. No significant overexpression of CXCL13 was observed in either of the sub-groups. Only N-cadherin fold change was significant in both sub-groups (Fig. 10A). All mRNAs except MMP2 are significantly overexpressed in both Oct4-M/H-TGF-β-L and Oct4-M/H-TGF-β-H sub-groups (Fig. 10B). MMP2 is not significant in Oct4-M/H-TGF-β-L tissues ($p = 0.05$).

3. Discussion

In spite of the current advancements in cancer therapeutics, high mortality rates due to BCa remain a concern and majority of these mortalities occur as a result of metastasis [65]. EMT is a complex process which is regulated through multiple signaling pathways, such as TGF-β signaling pathway [10–14]. In the TGF-β canonical pathway, phosphorylated Smad3 and Smad2 forms heterodimer with Smad4 and regulate transcription of several genes through interaction with regulatory DNA elements [66]. Recent research indicated that Smad3 regulates transcription of some genes in conjunction with some other TFs [39–41,67], like Oct4 [39,40].

Oct4 is a well-known CSC-related TF [68,69]. However, it is also associated with regulatory function in non-stem cancer cells [70]. Thus, a study correlating TGF-β and Oct4 to address possible connections between them has been desirable. We investigated a possible mechanism of interplay between the two molecules to regulate EMT during BCa. There is lack of comprehensive understanding of how TGF-β favors BCa progression only when cancer is in its advanced stages [14]. This study demonstrates that TGF-β-induction elevates Oct4 expression in BCa cells (Fig. 2). Significantly, TGF-β-induced-Oct4-overexpression is not restricted to CSCs (Fig. 3). In a significant proportion of patient samples, primary tumors with high TGF-β also express elevated Oct4 (Fig. 1; Supplementary Fig. S6). Further, TGF-β signaling and Oct4, not only induce EMT-regulators Snail and Slug expression individually, but also operate them synergistically (Fig. 4). Earlier literature has established that TGF-β induces increased migration and invasion of BCa cells [71,72]. In the present study, we demonstrated that Oct4-overexpression is associated with significant increase in migration and chemotactic invasion abilities of BCa cells. Increased MMP2, MMP9 activities are indicative of possible augmentation of ECM degradation (Fig. 5).

Notably, CXCL13-CXCR5 ligand-receptor pair is co-expressed within a significant proportion of primary tumor tissues from LNM-positive BCa patients and favors EMT [47,53]. We report that in absence of

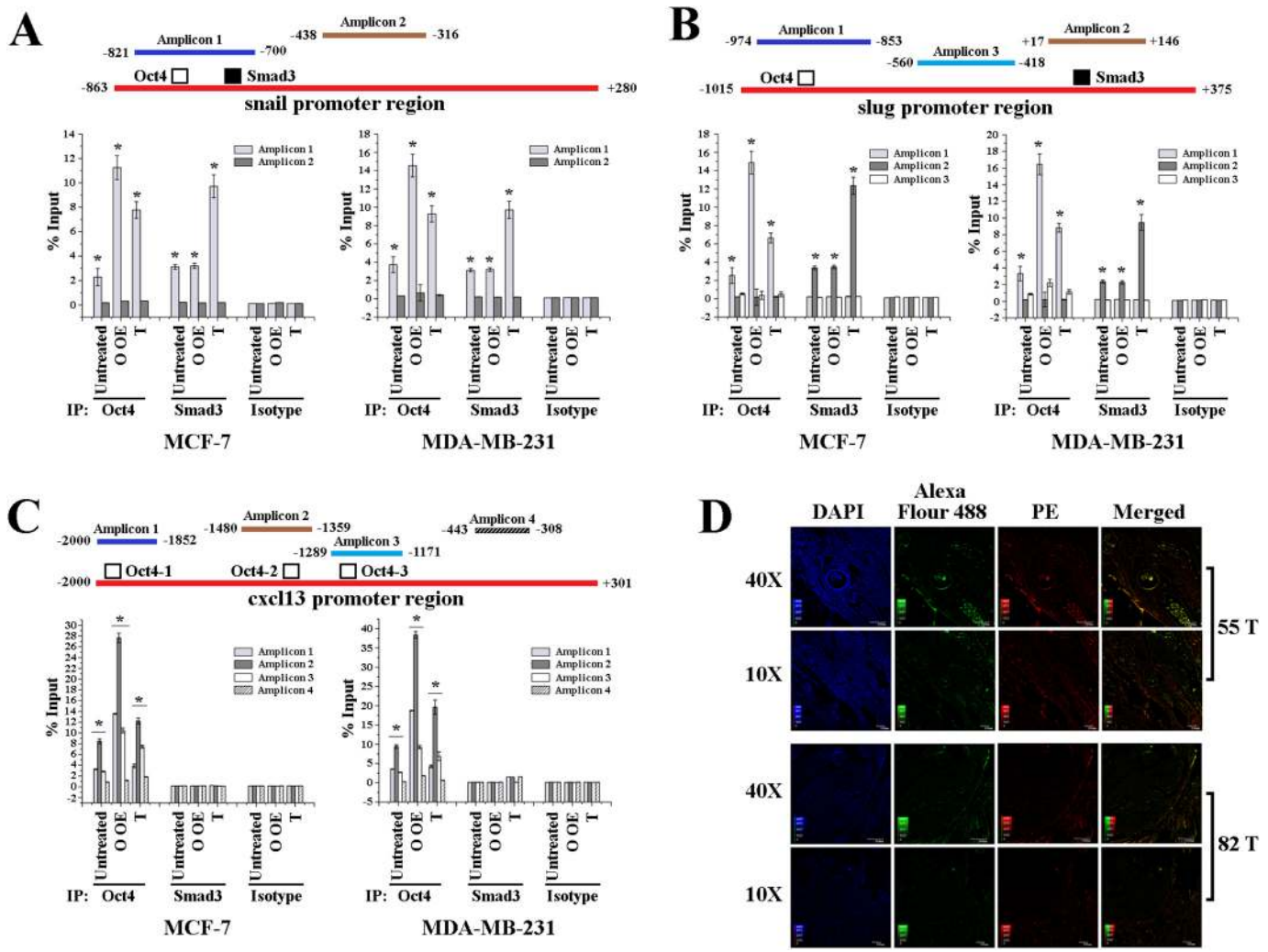

Fig. 9. Analyses of *in vivo* binding of Oct4 and Smad3 to the promoter regions of snail, slug and cxcl13 by ChIP.
(A) Map of the snail promoter showing predicted Oct4 and Smad3 binding sites and PCR products to be amplified in ChIP assay (upper panel). IP-cross-linked DNA fragments of snail promoter from anti-Oct4, anti-Smad3, isotype-IgG and input samples were amplified by qRT-PCR and percentage input were calculated from C_T values, represented as bar graphs (lower panel). (B) Map of slug promoter showing predicted Oct4 and Smad3 binding sites and PCR products amplified in ChIP assay (upper panel). IP-cross-linked DNA fragments of slug promoter from anti-Oct4, anti-Smad3, isotype-IgG and input samples were amplified by qRT-PCR and percentage input were calculated from C_T values, represented as bar graphs (lower panel). (C) Map of cxcl13 promoter showing predicted Oct4 binding sites and PCR products amplified in ChIP assay (upper panel). IP-cross-linked DNA fragments of cxcl13 promoter from anti-Oct4, anti-Smad3, isotype-IgG and input samples were amplified by qRT-PCR and percentage input calculated from C_T values are represented as bar graphs (lower panel). T represents cells treated with 1.0 ng/mL recombinant TGF-β1. O OE represents cells transfected for Oct4 overexpression, S si represents cells transfected with Smad3 siRNA, O si represents cells transfected with Oct4 siRNA (D) Immunofluroescence analyses of Oct4 (PE) and Smad3 (Alexa Fluor488) in representative primary tumor tissue sections from two late staged patients. 55 T and 82 T are primary tumor collected from patient serial no. 55 and 82, respectively. Images were captured in Olympus Fluoview FV1200 at 400× magnification. Results are representative of three independent experiments performed in triplicate and are represented as mean ± SEM. One-way ANOVA with Bonferroni correction was performed to assess statistical significance, where $^*p \leq 0.05$.

Oct4, TGF-β represses CXCL13 expression, which may be related to the fact that, Oct4 and Smad3 forms a heterodimer in the presence of Oct4. This perhaps inhibits Smad3 from executing the inhibitory function of TGF-β signaling on CXCL13 expression. Additionally, we demonstrate that Oct4 induces cxcl13 transcription through direct binding to specific sequences within cxcl13 promoter. Therefore, it could be inferred that Oct4 acts as a positive regulator of CXCL13 and simultaneously inhibits TGF-β-mediated-suppression of CXCL13 expression by forming heterodimers with Smad3. We also predict that the target of Smad3 for CXCL13 repression may be located at a distant chromosomal position, which means that Smad3-Oct4 heterodimers cannot bind cooperatively to these sites.

Further, we identified regions in snail and slug promoters for Smad3 and Oct4 binding (Figs. 6 and 9). Snail is known to be the transcriptional repressor of E-cadherin [73]. We observed that increased Snail expression is associated with loss of E-cadherin expression. These results support the hypothesis of Oct4-Smad3-co-occupancy on regulatory sequences of Snail and Slug. Oct4 and Smad3 binding sites are closely located (20 bases) in the snail promoter (Supplementary Fig. S2), while, the sites are distantly located (997 bases) in the slug promoter (Supplementary Fig. S3). Given that Smad3 forms heterodimers with Oct4, there would be decrease in available free Smad3 that could bind to distantly located sites or sequences on different chromosomes. However, we hypothesize that due to high level of chromosome compaction, Smad3 and Oct4 binding sites on the slug promoter may become very close to each other.

Percentage of Oct4-M/H samples (85.25%) among the LS patients ($n = 61$) is significantly higher than (26.74%) the ES patients ($n = 86$). Conversely, the percentage of Oct4-N/L samples (14.75%) among the LS patients is significantly lower than (73.26%) the ES patients.

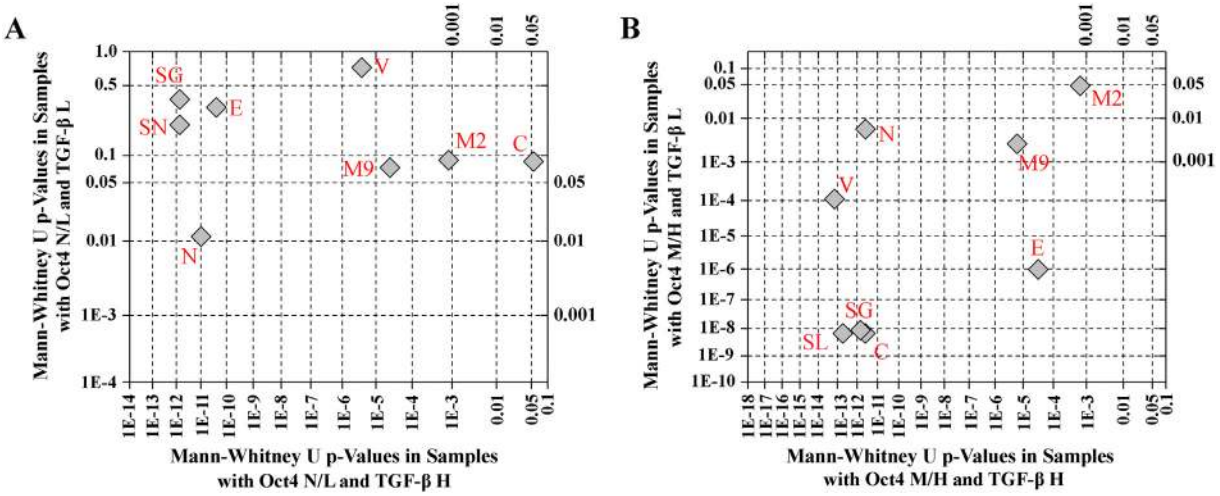

Fig. 10. Scatter plot showing statistical correlation of relative gene expressions in tumor or healthy tissues between sample groups having differential expression of Oct4 and TGF-β.

Scatter plot showing statistical correlation of Snail, Slug, Vimentin, E-cadherin, N-cadherin, MMP2, MMP9 and CXCL13 relative gene expression (tumor tissues/healthy tissues) between (A) Oct4 negative/low-TGF-β low and Oct4 negative/low-TGF-β high samples, as well as (B) Oct4 moderate/high-TGF-β low and Oct4 moderate/high-TGF-β high samples. Mann-Whitney *U* test-derived *p*-values from the four patient sub-groups are plotted. Regions of *p*-value ≥ 0.05, and < 0.05 were considered as not significant and significant, respectively.

However, percentages of TGF-β-H and TGF-β-L samples are quite equally distributed between ES (58.14% high and 41.68% low) and LS (59.02% high and 40.98% low) (Supplementary Fig. S7).

Therefore, in the LS, probability of Oct4 expression at M/H level is more than in the ES, which means there will be relatively higher Oct4-Smad3 heterodimerization in the LS. Higher the dimerization, higher will be the withdrawal of TGF-β-mediated-suppression of CXCL13 expression, which will eventually lead to higher CXCL13 level in the LS. Correspondingly, in ES, as percentage of Oct4-M/H samples is relatively low, there will be lower heterodimer formation and TGF-β will function to suppress CXCL13 expression. This hypothesis (Graphical abstract) could provide one possible answer to explain the discrepancy of TGF-β function in the BCa ES and LS.

From a clinical viewpoint, TGF-β and Oct4-co-expression within primary breast tumors could be used as a poor prognosis marker for BCa, although validation of this hypothesis requires future investigation using a larger sample number. In conclusion, Oct4-depletion or inhibition may be a plausible therapeutic strategy for BCa.

4. Materials and methods

4.1. Patient samples

Primary tumor and associated healthy tissues were collected from 147 BCa patients, with infiltrating duct carcinoma, who underwent MRM surgery at Saroj Gupta Cancer Centre and Research Institute (SGCC&RI), Kolkata, India. This study obtained institutional ethics committee permission [ECR/250/Inst/WB/2013] and informed consents were taken from all patients. Staging and grading of tumor samples were done by UICC-TNM classification [74] and RB protocol, respectively [75].

4.2. Cell lines, culture and treatment

BCa cell lines MCF7 and MDA-MB-231, and immortalized normal breast cell line MCF10A were procured from National Centre for Cell Science, Pune, India. BCa cell lines were routinely cultured in DMEM, supplemented with 10% FBS, 100 U/mL PenStrep, and maintained at 37 °C in a humidified-CO_2 incubator. For MCF10A, medium was additionally supplemented with insulin (10 μg/mL), cholera toxin (100 ng/mL) and EGF (20 ng/mL). Plasmid DNA or siRNA were transfected using Lipofectamine®3000. For TGF-β-stimulation, cells were treated with recombinant human TGF-β1 at laboratory-optimized concentrations (0.5 and 1.0 ng/mL). Transfection was done 2 h before TGF-β treatment. Both transfected and untransfected cell lines were cultured for 24 h in 2% FBS-medium.

4.3. RNA isolation, reverse-transcription, genomic DNA isolation and PCR

RNA was extracted using TRIzol reagent according to standard protocol [53] and reverse-transcribed into cDNA using MMLV reverse transcriptase. Genomic DNA was isolated using genomic DNA purification kit. PCR were performed to analyze mRNA expression and target amplification for cloning. End-point and qPCR were performed using Taq-master mix and SYBR-Green master mix, respectively. 18S rRNA was used as internal control. Primer sequences are listed in Supplementary Table S2. Fold changes in qPCR have been represented as relative values normalized to control and quantified in the terms of $2_{\mathrm{T}}^{-\Delta\Delta C}$. Experiments were performed thrice in triplicates.

4.4. Flow cytometry

Tissues were digested using Collagenase/Hyaluronidase cocktail overnight at 37 °C. Single cell suspensions (1×10^6) were incubated with fluorochrome-conjugated antibodies with appropriate isotype controls. Fc-blocker was used to minimize non-specific antibody binding (Supplementary Tables S3 and S4). Experiments were performed with appropriate controls. Analyses were done using BD-AccuriC6 software.

4.5. Bioinformatics analyses

Promoter sequences for snail (GRCh38.p7: 49982113-49983256), slug (GRCh38.p7: c48922455-48921065) and cxcl13 (GRCh37.p13: 78430907-78433207) genes were obtained from the official website of National Centre for Biotechnology Information (NCBI). Probable TFs and their putative binding sites within the promoter regions were predicted using the online tool Mapper2.0. Protein-protein blasts were performed using NCBI-Basic Local Alignment Search Tool (NCBI-BLAST) tool.

4.6. Molecular cloning

Coding sequence of Oct4 and promoter regions of snail, slug and cxcl13 along with their deletion variants were PCR-amplified from MDA-MB-231 cDNA and genomic DNA, respectively using Q5-high fidelity DNA polymerase, and specific primer pairs (Supplementary Tables S2 and S3). Mammalian expression vector pcDNA3.1(+) was used for Oct4 cloning and pGL3 basic reporter vector for promoter deletion variants. Both Oct4 clone (Supplementary Fig. S8) and all of the promoter variants were confirmed by restriction digestion and PCR amplification.

4.7. Western blot

Denatured total proteins were resolved in SDS-PAGE gels and immunoblotted in PVDF membranes overnight at 4 °C with primary antibodies followed by 2 h incubation with HRP-conjugated secondary antibodies at room temperature (RT) (Supplementary Table S3 and S4) and developed using luminal substrate. Experiments were performed in triplicates.

4.8. Luciferase assay

Both cell lines were transfected with different pGL3-promoter variants of snail, slug and cxcl13 along with different treatment combinations. qPCR-quantified luciferase mRNA fold change was considered as indicator of relative promoter activity, while, transfection with empty pGL3 vector as control (Supplementary Table S2).

4.9. Co-immunoprecipitation

Proteins (about 100 μg) from transfected cell lysates were incubated with anti-Oct4 or anti-Smad3 antibodies overnight at 4 °C (Supplementary Tables S3 and S4) followed by immunoprecipitation using proteinA/G-sepharose bead slurry. The antigen-antibody complex was eluted from the beads and analyzed by WB.

4.10. Chromatin immunoprecipitation

Conventional ChIP was performed using Millipore-17-295 kit according to recommended protocol. Sonicated cross-linked protein-DNA complexes were incubated with ChIP-grade antibodies (anti-Oct4, anti-Smad3), and precipitated with ProteinA-Agarose/Salmon sperm DNA. After eluting protein-DNA complexes and DNA purification, target DNA was quantified by qPCR (Supplementary Table S2).

4.11. Chemotactic invasion assay

To demonstrate chemotactic invasion of BCa cells, agarose spot assay for directed cell migration was performed. Conditioned medium with or without CCL5 was mixed with low-melting agarose to final concentration of 25 ng/mL. 4–5 agarose spots were placed on each of the sterile glass coverslips, placed in each well of a 6-well tissue culture plate and left at 4 °C for 5 mins to allow agarose spots solidify. Cell-front inside the agarose spots were monitored and captured at both 0 h and 24 h with a phase-contrast microscope.

4.12. Wound healing assay

Untreated and Oct4-overexpressing cells (confluency > 90%) in 6-well plates, were scratch-wounded using sterile micro-tip and incubated for 24 h in 2% FBS-medium. Wounded monolayer cells were washed thrice by PBS. Wound closure was monitored and captured at both 0 h and 24 h with a phase-contrast microscope.

4.13. Gelatin zymography

Gelatin zymography was performed in 10% SDS-PAGE, containing 0.1% gelatin under non-reducing conditions to determine the enzymatic activity of MMP2 and MMP9 in native proteins from MCF7 and MDA-MB-231 cell lines, using standard protocol[53].

4.14. Immunofluorescence

BCa cells (8×10^4) were seeded onto sterile coverslips in 6-well plates (confluency:80%) and treated with recombinant TGF-β1 (0.5 and 1.0 ng/mL) for 24 h. The next day, cells were fixed, permeabilized, blocked and incubated with PE-anti-Oct4 overnight at 4 °C. Nuclei were counterstained with DAPI (1 μg/mL).

Tissue sections were also incubated overnight at 4 °C with primary antibodies: PE-anti-Oct4 and anti-Smad3 together, while incubated with Alexa Fluor488-conjugated anti-rabbit secondary antibody against anti-Smad3 antibody at RT for 2 h (Supplementary Table S4).

4.15. Immunohistochemistry (IHC)

Immunohistochemistry (IHC) for TGF-β, Oct4 and CXCL13 were performed on formalin-fixed, paraffin-embedded tissue sections of 3–5 μM with standard protocol [53]. The sections were incubated with primary antibodies overnight at 4 °C and developed using DAB chromogen system and counterstained with hematoxylin (Supplementary Tables S3 and S4). The protein levels were scored negative, weak, moderate, and high according to expressions, respectively, after three independent observations.

4.16. Enzyme linked immuno-sorbent assay (ELISA)

To quantitatively measure the amount of CXCL13 in cell lysates, Sandwich ELISA was performed according to manufacturer's instructions using an ELISA kit and absorbance of the colored product was acquired using an ELISA reader at 450 nm (Supplementary Table S3). The sensitivity threshold of the test was 1.5 pg/mL.

4.17. Statistical analyses

Association between gene expression and clinicopathological characteristics was analyzed by Fisher's exact test. Distribution of variables was tested by Kolmogorov-Smirnov test. Mann-Whitney *U* test was performed to examine differences in fold change of gene expressions between healthy tissues and tumor tissues in different patient groups. One-way analysis of variance (ANOVA) (Bonferroni correction) was performed to assess the level of significance among paired data sets. Statistical analyses were performed using OriginPro8. All data are presented as mean ± SD and p-value of ≤ 0.05 was considered statistically significant.

Supplementary data to this article can be found online at https://doi.org/10.1016/j.bbadis.2018.03.010.

Author contributions

GM, SB and AB designed the study and planned the experiments. The majority of the experiments were performed by GM and SB, while SP, PK and SC also contributed towards completion of experiments. GM and SB designed and constructed all the clones of human gene and deletion constructs of promoter regions of genes. GM, SB, SRC, SP, AC, JDM, ALE and AB participated in analyzing and interpreting the data and provided intellectual input and critique to the study. AG helped us to acquire tumor samples needed for the study of the breast cancer patients from Saroj Gupta Cancer Centre and Research Institute and PKM helped us to procure and analyze the pathological data of the same patients. GM, SB, ALE and AB drafted the manuscript. All the authors

revised the manuscript thoroughly and approved the final version of the manuscript.

Conflict of interest

The authors declare no conflicts of interest.

Transparency document

The http://dx.doi.org/10.1016/j.bbadis.2018.03.010 associated with this article can be found, in online version.

Acknowledgements

This work was funded by Department of Science and Technology, Government of India [DST/INT/South Africa/P-06/2014] and South African National Research Foundation grant [UID-90753]. We thank all the patients who participated in this study and SGCC&RI nursing staffs and Shravasti Roy for their help in acquiring samples and clinico-pathological information of the patients respectively.

References

[1] A.J. Redig, S.S. McAllister, Breast cancer as a systemic disease: a view of metastasis, J. Intern. Med. 274 (2013) 113–126.
[2] L.A. Torre, F. Bray, R.L. Siegel, J. Ferlay, J. Lortet-Tieulent, A. Jemal, Global cancer statistics, 2012, CA Cancer J. Clin. 65 (2015) 87–108.
[3] U. Sen, R. Sankaranarayanan, S. Mandal, A.V. Ramanakumar, D.M. Parkin, M. Siddiqi, Cancer patterns in eastern India: the first report of the Kolkata cancer registry, Int. J. Cancer 100 (2002) 86–91.
[4] http://www.breastcancerindia.net/statistics/trends.html , Accessed date: 16 September 2016.
[5] P.D. Ottewell, L. O'Donnell, I. Holen, Molecular alterations that drive breast cancer metastasis to bone, Bonekey Rep 4 (2015) 643.
[6] J. Xu, S. Lamouille, R. Derynck, TGF-β-induced epithelial to mesenchymal transition, Cell Res. 19 (2009) 156–172.
[7] S. Lamouille, J. Xu, R. Derynck, Molecular mechanisms of epithelial–mesenchymal transition, Nat. Rev. Mol. Cell Biol. 15 (2014) 178–196.
[8] A. Barrallo-Gimeno, M.A. Nieto, The snail genes as inducers of cell movement and survival: implications in development and cancer, Development 132 (2005) 3151–3161.
[9] A. Dhasarathy, D. Phadke, D. Mav, R.R. Shah, P.A. Wade, The transcription factors snail and slug activate the transforming growth factor-Beta signaling pathway in breast cancer, PLoS One 6 (2011) e26514.
[10] M.F. Pang, A.M. Georgoudaki, L. Lambut, J. Johansson, V. Tabor, K. Hagikura, et al., TGF-β1-induced EMT promotes targeted migration of breast cancer cells through the lymphatic system by the activation of CCR7/CCL21-mediated chemotaxis, Oncogene 35 (2016) 748–760.
[11] C.H. Heldin, M. Landström, A. Moustakas, Mechanism of TGF-beta signaling to growth arrest, apoptosis, and epithelial-mesenchymal transition, Curr. Opin. Cell Biol. 21 (2009) 166–176.
[12] J. Massague, TGF beta in cancer, Cell 134 (2008) 215–230.
[13] P. Papageorgis, TGF-β signaling in tumor initiation, epithelial-to-mesenchymal transition, and metastasis, J. Oncol. 2015 (2015) 587193.
[14] J.M. Zarzynska, Two faces of TGF-Beta1 in breast cancer, Mediat. Inflamm. 2014 (2014) 141747.
[15] M. Geertz, S.J. Maerkl, Experimental strategies for studying transcription factor–DNA binding specificities, Brief. Funct. Genomics 9 (2010) 362–373.
[16] N.M. Luscombe, S.E. Austin, H.M. Berman, J.M. Thornton, An overview of the structures of protein-DNA complexes, Genome Biol. 1 (2000) (REVIEWS001).
[17] M.A. Velasco-Velázquez, V.M. Popov, M.P. Lisanti, R.G. Pestell, The role of breast cancer stem cells in metastasis and therapeutic implications, Am. J. Pathol. 179 (2011) 2–11.
[18] S.Q. Geng, A.T. Alexandrou, J.J. Li, Breast cancer stem cells: multiple capacities in tumor metastasis, Cancer Lett. 349 (2014) 1–7.
[19] C. Sheridan, H. Kishimoto, R.K. Fuchs, S. Mehrotra, P. Bhat-Nakshatri, C.H. Turner, et al., CD44 + /CD24-breast cancer cells exhibit enhanced invasive properties: an early step necessary for metastasis, Breast Cancer Res. 8 (2006) R59.
[20] R. Kim, J.S. Nam, OCT4 expression enhances features of cancer stem cells in a mouse model of breast cancer, Inst. Lab. Anim. Res. J. 27 (2011) 147–152.
[21] M. Boiani, H.R. Schöler, Regulatory networks in embryo-derived pluripotent stem cells, Nat. Rev. Mol. Cell Biol. 6 (2005) 872–884.
[22] M. Pesce, X. Wang, D.J. Wolgemuth, H. Schöler, Differential expression of the Oct-4 transcription factor during mouse germ cell differentiation, Mech. Dev. 71 (1998) 89–98.
[23] Y. Atlasi, S.J. Mowla, S.A. Ziaee, P.J. Gokhale, P.W. Andrews, OCT4 spliced variants are differentially expressed in human pluripotent and nonpluripotent cells, Stem Cells 26 (2008) 3068–3074.
[24] M. Pesce, H.R. Schöler, Oct-4: gatekeeper in the beginnings of mammalian development, Stem Cells 19 (2001) 271–278.
[25] G.Q. Ling, D.B. Chen, B.Q. Wang, L.S. Zhang, Expression of the pluripotency markers Oct3/4, Nanog and Sox2 in human breast cancer cell lines, Oncol. Lett. 4 (2012) 1264–1268.
[26] X. Yin, B.H. Zhang, S.S. Zheng, D.M. Gao, S.J. Qiu, W.Z. Wu, et al., Coexpression of gene Oct4 and Nanog initiates stem cell characteristics in hepatocellular carcinoma and promotes epithelial-mesenchymal transition through activation of Stat3/snail signaling, J. Hematol. Oncol. 8 (2015) 23.
[27] Y. Atlasi, S.J. Mowla, S.A. Ziaee, A.R. Bahrami, OCT-4, an embryonic stem cell marker, is highly expressed in bladder cancer, Int. J. Cancer 120 (2007) 1598–1602.
[28] L. Liu, J. Zhang, C. Fang, Z. Zhang, Y. Feng, X. Xi, OCT4 mediates FSH-induced epithelial-mesenchymal transition and invasion through the ERK1/2 signaling pathway in epithelial ovarian cancer, Biochem. Biophys. Res. Commun. 461 (2015) 525–532.
[29] U.I. Ezeh, P.J. Turek, R.A. Reijo, A.T. Clark, Human embryonic stem cell genes OCT4, NANOG, STELLAR, and GDF3 are expressed in both seminoma and breast carcinoma, Cancer 104 (2005) 2255–2265.
[30] S.M. Kumar, S. Liu, H. Lu, H. Zhang, P.J. Zhang, P.A. Gimotty, et al., Acquired cancer stem cell phenotypes through Oct4-mediated dedifferentiation, Oncogene 31 (2012) 4898–4911.
[31] J. Wen, J.Y. Park, K.H. Park, H.W. Chung, S. Bang, S.W. Park, et al., Oct4 and Nanog expression is associated with early stages of pancreatic carcinogenesis, Pancreas 39 (2010) 622–666.
[32] H.M. Meng, P. Zheng, X.Y. Wang, C. Liu, H.M. Sui, S.J. Wu, et al., Over-expression of Nanog predicts tumor progression and poor prognosis in colorectal cancer, Cancer Biol. Ther. 9 (2010) 295–302.
[33] D. Zeineddine, A.A. Hammoud, M. Mortada, H. Boeuf, The Oct4 protein: more than a magic stemness marker, Am. J. Stem Cells 3 (2014) 74–82.
[34] B.S. Koo, S.H. Lee, J.M. Kim, S. Huang, S.H. Kim, Y.S. Rho, et al., Oct4 is a critical regulator of stemness in head and neck squamous carcinoma cells, Oncogene 34 (2015) 2317–2324.
[35] S. Boumahdi, G. Driessens, G. Lapouge, S. Rorive, D. Nassar, M. Le Mercier, et al., SOX2 controls tumour initiation and cancer stem-cell functions in squamous-cell carcinoma, Nature 511 (2014) 246–250.
[36] K. Abubaker, R.B. Luwor, H. Zhu, O. McNally, M.A. Quinn, C.J. Burns, et al., Inhibition of the JAK2/STAT3 pathway in ovarian cancer results in the loss of cancer stem cell-like characteristics and a reduced tumor burden, BMC Cancer 14 (2014) 317.
[37] M. Pucéat, TGF beta in the differentiation of embryonic stem cells, Cardiovasc. Res. 74 (2007) 256–261 (e-pub ahead of print 16 December 2006).
[38] H.K. Au, J.H. Chang, Y.C. Wu, Y.C. Kuo, Y.H. Chen, W.C. Lee, et al., TGF-βI regulates cell migration through pluripotent transcription factor OCT4 in endometriosis, PLoS One 10 (2015) e0145256.
[39] A.C. Mullen, D.A. Orlando, J.J. Newman, J. Lovén, R.M. Kumar, S. Bilodeau, et al., Master transcription factors determine cell-type-specific responses to TGF-β signaling, Cell 147 (2011) 565–576.
[40] C. Hadjimichael, K. Chanoumidou, N. Papadopoulou, P. Arampatzi, J. Papamatheakis, A. Kretsovali, Common stemness regulators of embryonic and cancer stem cells, World J. Stem Cells 7 (2015) 1150–1184.
[41] J. Massagué, Q. Xi, TGF-β control of stem cell differentiation genes, FEBS Lett. 586 (2012) 1953–1958.
[42] L. Chen, Z. Huang, G. Yao, X. Lyu, J. Li, X. Hu, et al., The expression of CXCL13 and its relation to unfavorable clinical characteristics in young breast cancer, J. Transl. Med. 13 (2015) 168.
[43] C.H. Jenh, M.A. Cox, W. Hipkin, T. Lu, C. Pugliese-Sivo, W. Gonsiorek, et al., Human B cell-attracting chemokine 1 (BCA-1; CXCL13) is an agonist for the human CXCR3 receptor, Cytokine 15 (2001) 113–121.
[44] M.D. Gunn, V.N. Ngo, K.M. Ansel, E.H. Ekland, J.G. Cyster, L.T. Williams, A B-cell-homing chemokine made in lymphoid follicles activates Burkitt's lymphoma receptor-1, Nature 391 (1998) 799–803.
[45] J.L. Vissers, F.C. Hartgers, E. Lindhout, C.G. Figdor, G.J. Adema, BLC (CXCL13) is expressed by different dendritic cell subsets *in vitro* and *in vivo*, Eur. J. Immunol. 31 (2001) 1544–1549.
[46] H.S. Carlsen, E.S. Baekkevold, H.C. Morton, G. Haraldsen, P. Brandtzaeg, Monocyte-like and mature macrophages produce CXCL13 (B cell-attracting chemokine 1) in inflammatory lesions with lymphoid neogenesis, Blood 104 (2004) 3021–3027.
[47] A. Panse, K. Friedrichs, A. Marx, Y. Hildebrandt, T. Luetkens, K. Barrels, et al., Chemokine CXCL13 is overexpressed in the tumour tissue and in the peripheral blood of breast cancer patients, Br. J. Cancer 99 (2008) 930–938.
[48] C. Havenar-Daughton, M. Lindqvist, A. Heit, J.E. Wu, S.M. Reiss, K. Kendric, et al., CXCL13 is a plasma biomarker of germinal center activity, Proc. Natl. Acad. Sci. U. S. A. 113 (2016) 2702–2707.
[49] C.D. Allen, K.M. Ansel, C. Low, R. Lesley, H. Tamamura, N. Fujii, et al., Germinal center dark and light zone organization is mediated by CXCR4 and CXCR5, Nat. Immunol. 5 (2004) 943–952 (e-pub ahead of print 1 August 2004).
[50] J. Meijer, I.S. Zeelenberg, B. Sipos, E. Roos, The CXCR5 chemokine receptor is expressed by carcinoma cells and promotes growth of colon carcinoma in the liver, Cancer Res. 66 (2006) 9576–9582.
[51] I. Airoldi, C. Cocco, F. Morandi, I. Prigione, V. Pistoia, CXCR5 may be involved in the attraction of human metastatic neuroblastoma cells to the bone marrow, Cancer Immunol. Immunother. 57 (2008) 541–548.
[52] C.P. El Haibi, P.K. Sharma, R. Singh, P.R. Johnson, J. Suttles, S. Singh, et al., PI3Kp110-, Src-, FAK-dependent and DOCK2-independent migration and invasion of CXCL13-stimulated prostate cancer cells, Mol. Cancer 9 (2010) 85.
[53] S. Biswas, S. Sengupta, S. Roy Chowdhury, S. Jana, G. Mandal, P.K. Mandal, et al., CXCL13-CXCR5 co-expression regulates epithelial to mesenchymal transition of

breast cancer cells during lymph node metastasis, Breast Cancer Res. Treat. 143 (2014) 265–276.
[54] A. Manzo, B. Vitolo, F. Humby, R. Caporali, D. Jarrossay, F. Dell'accio, et al., Mature antigen-experienced T helper cells synthesize and secrete the B cell chemoattractant CXCL13 in the inflammatory environment of the rheumatoid joint, Arthritis Rheum. 58 (2008) 3377–3387.
[55] S. Kobayashi, K. Murata, H. Shibuya, M. Morita, M. Ishikawa, M. Furu, et al., A distinct human CD4+ T cell subset that secretes CXCL13 in rheumatoid synovium, Arthritis Rheum. 65 (2013) 3063–3072.
[56] S. Kobayashi, T. Watanabe, R. Suzuki, M. Furu, H. Ito, J. Ito, et al., TGF-β induces the differentiation of human CXCL13-producing CD4(+) T cells, Eur. J. Immunol. 46 (2016) 360–371.
[57] D. Zeineddine, E. Papadimou, K. Chebli, M. Gineste, J. Liu, C. Grey, et al., Oct-3/4 dose dependently regulates specification of embryonic stem cells toward a cardiac lineage and early heart development, Dev. Cell 11 (2006) 535–546.
[58] M.M. Burdick, K.A. Henson, L.F. Delgadillo, Y.E. Choi, D.J. Goetz, D.F. Tees, et al., Expression of E-selectin ligands on circulating tumor cells: cross-regulation with cancer stem cell regulatory pathways? Front. Oncol. 2 (2012) 103.
[59] J. Hu, K. Qin, Y. Zhang, J. Gong, N. Li, D. Lv, et al., Downregulation of transcription factor Oct4 induces an epithelial-to-mesenchymal transition via enhancement of Ca2+ influx in breast cancer cells, Biochem. Biophys. Res. Commun. 411 (2011) 786–791.
[60] Y.J. Wang, M. Herlyn, The emerging roles of Oct4 in tumor-initiating cells, Am. J. Phys. Cell Physiol. 309 (2015) C709–18.
[61] P. Lu, K. Takai, V.M. Weaver, Z. Werb, Extracellular matrix degradation and remodeling in development and disease, Cold Spring Harb. Perspect. Biol. 3 (2011) a005058 (pii).
[62] F.A. Venning, L. Wullkopf, J.T. Erler, Targeting ECM disrupts cancer progression, Front. Oncol. 5 (2015) 224.
[63] K. Kessenbrock, V. Plaks, Z. Werb, Matrix metalloproteinases: regulators of the tumor microenvironment, Cell 141 (2010) 52–67.
[64] M.J. Duffy, T.M. Maguire, A. Hill, E. McDermott, N. O'Higgins, Metalloproteinases: role in breast carcinogenesis, invasion and metastasis, Breast Cancer Res. 2 (2000) 252–257.
[65] P. Mehlen, A. Puisieux, Metastasis: a question of life or death, Nat. Rev. Cancer 6 (2006) 449–458.
[66] M. Pickup, S. Novitskiy, H.L. Moses, The roles of TGFβ in the tumour microenvironment, Nat. Rev. Cancer 13 (2013) 788–799.
[67] T. Gaarenstroom, C.S. Hill, TGF-β signaling to chromatin: how Smads regulate transcription during self-renewal and differentiation, Semin. Cell Dev. Biol. 32 (2014) 107–118.
[68] S. Kaufhold, H. Garbán, B. Bonavida, Yin Yang 1 is associated with cancer stem cell transcription factors (SOX2, OCT4, BMI1) and clinical implication, J. Exp. Clin. Cancer Res. 35 (2016) 84.
[69] S. Lee, S. Wottrich, B. Bonavida, Crosstalks between Raf-kinase inhibitor protein and cancer stem cell transcription factors (Oct4, KLF4, Sox2, Nanog), Tumour Biol. 39 (2017) 1010428317692253.
[70] D. Wang, P. Lu, H. Zhang, M. Luo, X. Zhang, X. Wei, et al., Oct-4 and Nanog promote the epithelial-mesenchymal transition of breast cancer stem cells and are associated with poor prognosis in breast cancer patients, Oncotarget 5 (2014) 10803–10815.
[71] H. Moses, M.H. Barcellos-Hoff, TGF-beta biology in mammary development and breast cancer, Cold Spring Harb. Perspect. Biol. 3 (2011) a003277.
[72] M.H. Barcellos-Hoff, R.J. Akhurst, Transforming growth factor-beta in breast cancer: too much, too late, Breast Cancer Res. 11 (2009) 202.
[73] H. Peinado, F. Portillo, A. Cano, Transcriptional regulation of cadherins during development and carcinogenesis, Int. J. Dev. Biol. 48 (2004) 365–375.
[74] J.D. Brierley, M.K. Gospodarowicz, C. Wittekind, TNM Classification of Malignant Tumours, Wiley-Blackwell, 2016 (ISBN: 978-1-119-26357-9, 264 pages).
[75] H.J. Bloom, W.W. Richardson, (1957) histological grading and prognosis in breast cancer; a study of 1409 cases of which 359 have been followed for 15 years, Br. J. Cancer 11 (1957) 359–377.